

Light Meson Decays from Photon-Induced Reactions with CLAS

Michael C. Kunkel^{1,a)}
For the CLAS Collaboration

¹*Forschungszentrum Jülich, Jülich (Germany)*

^{a)}m.kunkel@fz-juelich.de

Abstract. Photo-production experiments with the CEBAF Large Acceptance Spectrometer (CLAS) at the Thomas Jefferson National Laboratory produce data sets with unprecedented statistics for light mesons. With these data sets, measurements of transition form factors for η , ω , and η' mesons via conversion decays can be performed using the invariant mass distribution of the final state dileptons. Tests of fundamental symmetries and information on the light quark mass difference can be performed using a Dalitz plot analysis of the meson decay. An overview of the first results, from existing CLAS data, and future prospects within the newly upgraded CLAS12 apparatus are given.

INTRODUCTION

Decays of light mesons provide insight into the structure of the meson. The Light Meson Decay (LMD) group, established at the Thomas Jefferson National Facility with worldwide collaboration, investigates physics pertaining to, but not limited to, transition form factors, anomalous decays and the search for CP violation through Dalitz plot analysis. The presentation given was an overview of the LMD program, recent updates on measurements and an outlook on measurements that can be taken with the CLAS12 detector.

Light Meson Decay Program

The light meson group was established in 2013. The goal of the group is to investigate properties of light meson decays using data obtained with the CLAS detector. Figure 1 shows the CLAS detector and its components. Since decays of

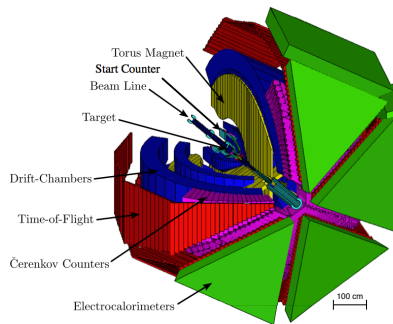


FIGURE 1: The CEBAF Large Acceptance Spectrometer (CLAS)

hadrons are independent of production, all CLAS data can be used, however there are two experiments that were chosen as flagships for the program, the g11 and g12 experiment. Both experiments use a photon beam incident on a liquid

hydrogen target which created photo-induced reactions with photon beam energies of 800 MeV - 3.8 GeV for g11 and 1.1 GeV - 5.5 GeV for g12. See [1] for a complete list of meson decays the LMD group plans to investigate.

The Radiative Decay of the η and η' Meson

The two-photon decay of the pseudoscalar mesons $\pi^0, \eta, \eta' \rightarrow \gamma\gamma$ proceed via the triangle or axial anomaly. Radiative decays of $\eta, \eta' \rightarrow \pi^+\pi^-\gamma$ are related to the box anomaly. The radiative decay widths of η' and η are determined by the box anomaly in the chiral limit by Equation 1;

$$\frac{d\Gamma(\eta^{(\prime)} \rightarrow \pi^+\pi^-\gamma)}{ds_{\pi\pi}} = A|P(s_{\pi\pi})F_V(s_{\pi\pi})\Gamma_0(s_{\pi\pi})| \quad (1)$$

where $\Gamma_0(s_{\pi\pi})$ is the P-wave phase-space constant, denoted in Equation 2 with κ being a numerical constant. $F_V(s_{\pi\pi})$ is the pion form factor that can be approximated by Equation 3 and $P(s_{\pi\pi})$ is expanded around the chiral limit, $s_{\pi\pi} = 0$, as in Equation 4, where α is the variable of measurement.

$$\Gamma_0(s_{\pi\pi}) = \frac{\kappa(M_{\eta^{(\prime)}}^2 - s_{\pi\pi})^3 s_{\pi\pi} \left(1 - \frac{4M_\pi^2}{s_{\pi\pi}}\right)^{\frac{3}{2}}}{M_{\eta^{(\prime)}}^3} \quad (2)$$

$$|F_V(s_{\pi\pi})| \approx 1 + (2.12 \pm 0.01)s_{\pi\pi} + (2.13 \pm 0.01)s_{\pi\pi}^2 + (13.89 \pm 0.14)s_{\pi\pi}^3 \quad (3)$$

$$P(s_{\pi\pi}) = 1 + \alpha s_{\pi\pi} + O(s_{\pi\pi}^2) \quad (4)$$

Previous results on the radiative decay for the η meson from WASA-at-COSY [2] and KLOE [3] would profit from further measurements. Only one measurement exists for the η' radiative decay [4]. With the CLAS g11 experiment, both the η and η' radiative decay width will be measured. In Figure 2 the CLAS g11 data is shown for the particle selection of exclusive $\gamma p \rightarrow p\pi^+\pi^-\gamma$. Selecting events within a 2.5σ range of $\eta^{(\prime)}$ the photon energy distribution, which is related to $s_{\pi\pi}$ by Equation 5, is shown in Figure 3.

$$s_{\pi\pi} = m^2 - 2E_\gamma m \quad (5)$$

Comparing the shape of the left Figure 3 to those of Figure 4, for the η meson, and also the right Figure 3 to that of

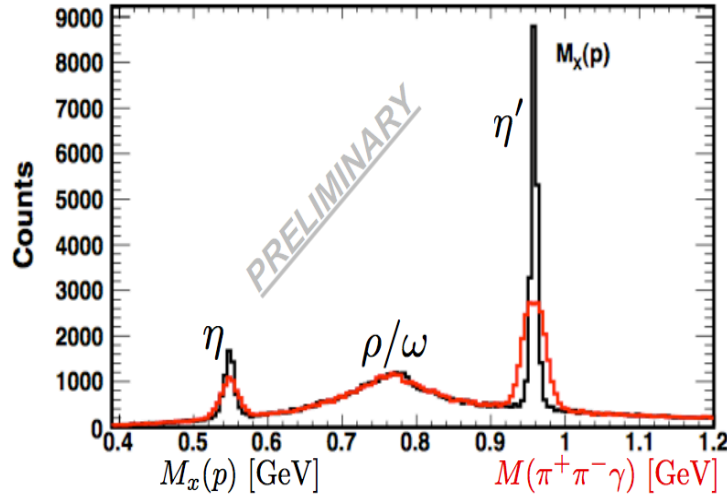


FIGURE 2: CLAS yield for $\gamma p \rightarrow p\eta^{(\prime)} \rightarrow p\pi^+\pi^-\gamma$ from the g11 data set

Figure 5, for the η' meson, it can be seen that the CLAS data is suitable for comparison with previous measurements.

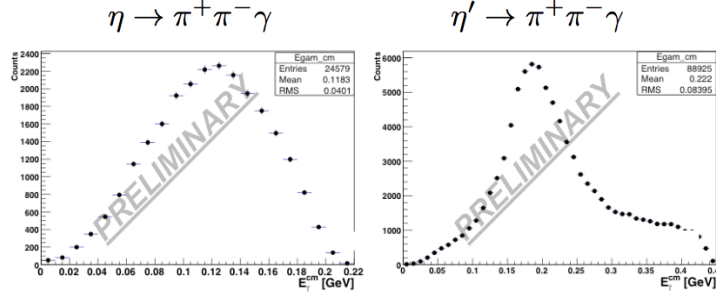


FIGURE 3: CLAS photon energy distribution for η (left) and η' (right)

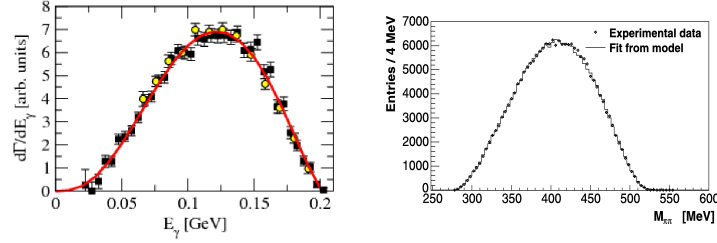


FIGURE 4: Left: Photon energy distribution for η with model [5], showing the WASA-at-COSY data [2] (solid symbols) and previous results from [6] (yellow symbols). Right: The KLOE photon energy distribution for η [3].

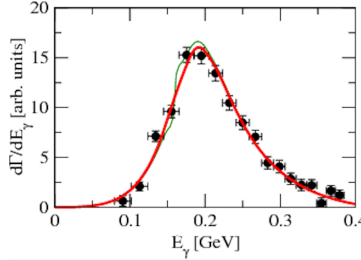


FIGURE 5: CRYSTAL BARREL photon energy distribution for η' [4]

The Transition Form Factor of the ω Meson

Transition form factors characterize modifications of the point-like photon-meson vertex due to the structure of the meson. The virtual photon can interact with quarks, therefore it can be used as a probe for the internal structure of mesons and its electromagnetic interaction is calculable with the Kroll-Wada formula [7], Equation 6;

$$\frac{d\Gamma_{M \rightarrow l^+ l^- X}}{dq^2 d\Gamma_{M \rightarrow X\gamma}} = \frac{\alpha}{3\pi q^2} \left(\left(1 + \frac{q^2}{m_M^2 - m_X^2} \right)^2 - \frac{4m_M^2 q^2}{(m_M^2 - m_X^2)^2} \right)^{\frac{3}{2}} \left(1 - \frac{4m_l^2}{q^2} \right)^{1/2} \left(1 + \frac{2m_l^2}{q^2} \right) \Big|_{\text{Q.E.D.}} \quad (6)$$

where M is the species of meson i.e. π^0 , η , ω , η' , etc., X is the child particle in the decay, m_M the mass of the meson, m_X the mass of the child particle, m_l the mass of the lepton species in the decay, i.e. e^\pm or μ^\pm and q being the momentum transfer which is identical to the invariant mass of the dilepton. Deviations of Equation 6 represent the internal structure of the meson for pseudoscalar mesons, while for vector mesons the deviation represents the transition from $M \rightarrow X$. These deviations are the transition form factor $|F(q^2)|$ and can be determined by comparing Equation 6 to what is measured experimentally.

$$\frac{d\Gamma_{M \rightarrow l^+ l^- X}}{dq^2 d\Gamma_{M \rightarrow X\gamma}} \Big|_{\text{measured}} = \frac{d\Gamma_{M \rightarrow l^+ l^- X}}{dq^2 d\Gamma_{M \rightarrow X\gamma}} \Big|_{\text{Q.E.D.}} |F(q^2)|^2 \quad (7)$$

Depending on the decay width of the meson of interest, the transition can be modeled as a simple pole, Equation 8, a complex pole, Equation 9, or some other function that describes the transition.

$$|F(q^2)| = \frac{1}{1 - \frac{q^2}{\Lambda^2}} \quad (8)$$

$$|F(q^2)|^2 = \frac{\Lambda^2(\Lambda^2 + \gamma^2)}{(\Lambda^2 - q^2)\Lambda^2\gamma^2}, \quad (9)$$

where Λ and γ is the mass and width of the virtual vector meson mass, respectively. Recent measurements of the transition form factor for $\omega \rightarrow \mu^+\mu^-\gamma$ have shown unexpected discrepancies with the Vector Dominance Model [8] and recent models of chiral Lagrangian field theory [9], and dispersion theory [10] attempt to predict the contributions of the virtual vector meson as seen in Figure 6.

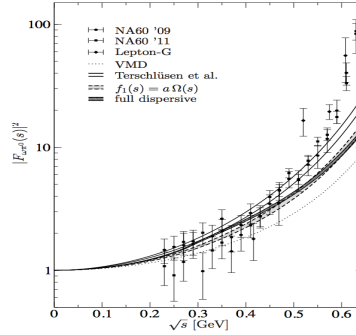


FIGURE 6: Form factor of the decay $\omega \rightarrow l^+l^-\gamma$ compared to dimuon data by the NA60 Collaboration [8, 11] and LEPS [12]. Shown are VMD (dotted line) Eqs. (6, 9) using the mass of the ρ meson as the virtual vector meson, the results of a chiral Lagrangian treatment with explicit vector mesons [9] (white shaded curve with solid borders), a simplified approximation to the full dispersive solution [10] (gray shaded curve with dashed borders), full dispersive solution [10] (black hatched curve with solid borders). [10]

With the CLAS g12 experiment, lepton (e^\pm) identification is done using Cherenkov detectors and electromagnetic calorimetry, providing a $e^+e^-/\pi^+\pi^-$ rejection of 10^6 . Using the e^\pm data from CLAS g12, the $\omega \rightarrow pe^+e^-\pi^0$ transition form factor can be extracted. Figure 7 shows the region of the ω meson. Also, the knowledge of the η form factor is

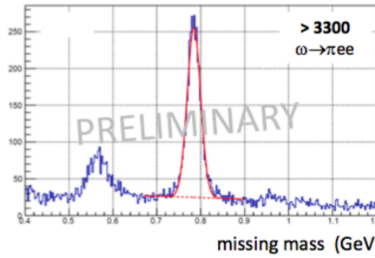


FIGURE 7: CLAS yield for $\gamma p \rightarrow pX \rightarrow pe^+e^-\pi^0$ from g12 data set

needed for the interpretation of the $(g_\mu - 2)/2$ uncertainty [13]. Furthermore, the ratio of the η and η' transition form factor provides information of the mixing angle of the combination of the singlet, η_0 , and nonet, η_8 , which are the components of the physical eigenstates, the η and η' meson.

Update on the Branching Ratio Measurement of the $\eta' \rightarrow e^+e^-\gamma$ Decay

A recent measurement of BESIII reports the branching ratio $\Gamma(\eta' \rightarrow e^+e^-\gamma)/\Gamma(\eta' \rightarrow \gamma\gamma)$ to be $2.13 \pm 0.09(stat.) \pm 0.07(sys.)10^{-2}$ from 864 events [14]. Using the e^\pm data from CLAS g12, preliminarily 89 events of the $\eta' \rightarrow e^+e^-\gamma$

decay were observed and analyzed, using the Q-factor [15] method to suppress background from neighboring $A \rightarrow e^+e^-X$ decays, Figure 8. A preliminary branching ratio $\Gamma(\eta' \rightarrow e^+e^-\gamma)/\Gamma(\eta' \rightarrow \gamma\gamma)$ was measured to be consistent

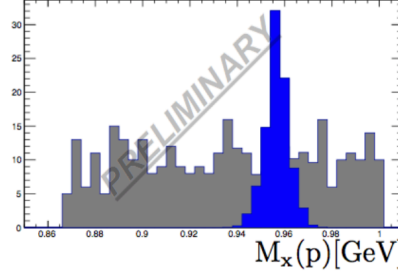


FIGURE 8: CLAS yield for $\gamma p \rightarrow p\eta' \rightarrow pe^+e^-\gamma$ from g12 data set. Blue peak represents the signal extracted using the Q-factor method, while the gray band represents the background.

with the BESIII measurement. However, the statistics of either BESIII or CLAS are not ample enough to determine, statistically, which theoretical model best represents the structure of the η' meson [16, 17, 18]. Table 1 outlines the current measurements and theoretical predictions.

TABLE 1: Current Measurements and Theoretical Predictions of the η' charge radius

Charge Radius $\langle r \rangle$	Measurement (M) / Prediction (P)
CLAS ($\eta' \rightarrow e^+e^-\gamma$)	TBD
BESIII ($\eta' \rightarrow e^+e^-\gamma$)	(M) $1.60 \pm 0.17(stat) \pm 0.08(sys) \text{GeV}^{-2}$ [14]
CELLO ($\eta' \rightarrow \mu^+\mu^-\gamma$)	(M) $1.7 \pm 0.4 \text{GeV}^{-2}$ [19]
Dispersion	(P) $1.53^{+0.15}_{-0.08} \text{GeV}^{-2}$ [18]
ChPT	(P) 1.6GeV^{-2} [17]
VMD	(P) 1.45GeV^{-2} [16]

Future Measurement of the η' Meson Transition Form Factor with CLAS12

With the newly built CLAS12 detector, e^\pm identification can be achieved with a $e^+e^-/\pi^+\pi^-$ rejection of $10^6 - 10^{11}$ while retaining $e^+e^-\gamma$ acceptance $\sim 1\% - 0.1\%$, Figure 9 depicts the CLAS12 detector and its subsystems. Using the GEant4 Monte-Carlo (GEMC) simulation suite for CLAS12, a simulation of $600,000 \text{ } ep \rightarrow e'\gamma^*p \rightarrow p\eta' \rightarrow pe^+e^-\gamma$ was performed. The generation of events included cross-section information obtained from previous CLAS measurements, the s^n scaling law on the cross-section and the VMD model for the decay of the η' meson to achieve a reasonable model of the production of the η' meson. The estimated quasi-real photon rate with the CLAS12 Forward Tagger are $5 \cdot 10^7 \gamma/s$ which will be impinged on a 5 cm ℓH_2 target. Count rates of $\eta' \rightarrow pe^+e^-\gamma$ were calculated for exclusive $\gamma p \rightarrow p\eta' \rightarrow pe^+e^-\gamma$ and inclusive $\gamma p \rightarrow \eta'(p) \rightarrow e^+e^-\gamma(p)$ with and without the electromagnetic calorimeter (EC) information for the e^+e^- pairs. For the exclusive reaction it was preliminarily estimated that the number of $\eta' \rightarrow e^+e^-\gamma$ decays to be detected within 100 days of beam time would be $\sim 22,000 - 2,400$, and the statistical uncertainty of the transition form factor measurement would be $\sim 0.3\% - 3\%$, with and without the EC information, respectively, Figure 10. For the inclusive reaction it was preliminarily estimated that the number of $\eta' \rightarrow pe^+e^-\gamma$ decays to be detected within 100 days of beam time would be $\sim 53,000 - 5,900$, and the statistical uncertainty of the transition form factor measurement would be $\sim 0.1\% - 1\%$, with and without the EC information, respectively, Figure 10. Furthermore, with the statistics estimated to be seen in CLAS12, a η' signal is expected in the complete range of $q = e^+e^-$, allowing for a measurement at the divergent part of the VMD model $q \sim m_\rho$.

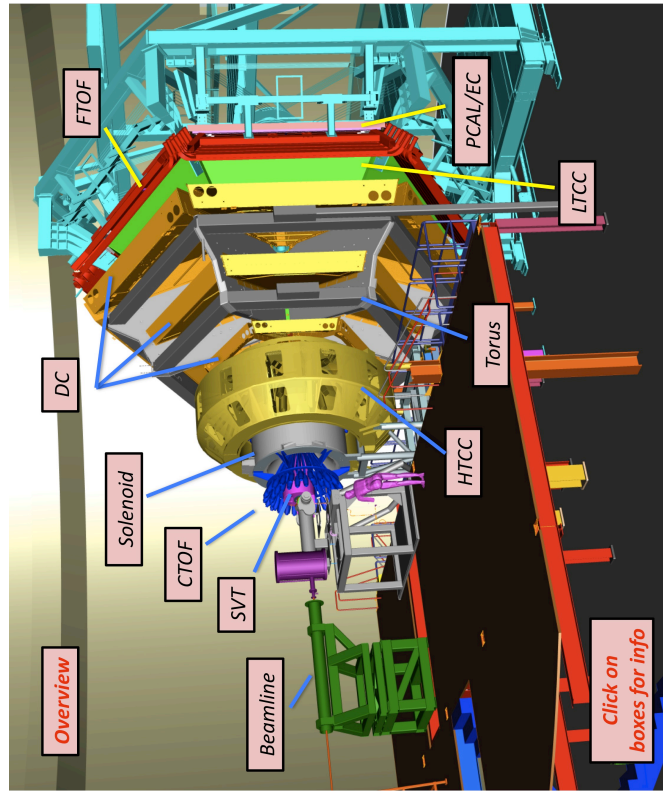


FIGURE 9: The CEBAF Large Acceptance Spectrometer (CLAS12)
(<https://www.jlab.org/Hall-B/clas12-web/>)

REFERENCES

- [1] M. Amarian *et al.*, *Photoproduction and Decay of Light Mesons in CLAS*.
- [2] P. Adlarson *et al.*, *Physics Letters B* **707**, 243 – 249 (2012).
- [3] D. Babusci *et al.*, *Physics Letters B* **718**, 910 – 914 (2013).
- [4] A. Abele *et al.*, *Physics Letters B* **402**, 195 – 206 (1997).
- [5] F. Stollenwerk *et al.*, *Physics Letters B* **707**, 184 – 190 (2012).
- [6] M. Gormley *et al.*, *Phys. Rev. D* **2**, 501–505 (1970).
- [7] N. M. Kroll and W. Wada, *Phys. Rev.* **98**, 1355–1359 (1955).
- [8] R. Arnaldi *et al.*, *Physics Letters B* **677**, 260 – 266 (2009).
- [9] C. Terschlusen and S. Leupold, *Physics Letters B* **691**, 191 – 201 (2010).
- [10] S. P. Schneider *et al.*, *Phys. Rev.* **D86**, p. 054013 (2012), arXiv:1206.3098 [hep-ph] .
- [11] G. Usai, *Nuclear Physics A* **855**, 189 – 196 (2011).
- [12] R. Dzhelyadin *et al.*, *Physics Letters B* **102**, 296 – 298 (1981).
- [13] T. Blum *et al.*, (2013), arXiv:1311.2198 [hep-ph] .
- [14] M. Ablikim *et al.* (BESIII), *Phys. Rev.* **D92**, p. 012001 (2015).
- [15] M. Williams *et al.*, *JINST* **4**, p. P10003 (2009).
- [16] A. Bramon and E. Mass, *Physics Letters B* **104**, 311 – 314 (1981).
- [17] L. Ametller *et al.*, *Phys. Rev. D* **45**, 986–989 (1992).
- [18] C. Hanhart *et al.*, *Eur. Phys. J.* **C73**, p. 2668 (2013), arXiv:1307.5654 [hep-ph] .
- [19] R. Dzhelyadin *et al.*, *Physics Letters B* **88**, 379 – 380 (1979).

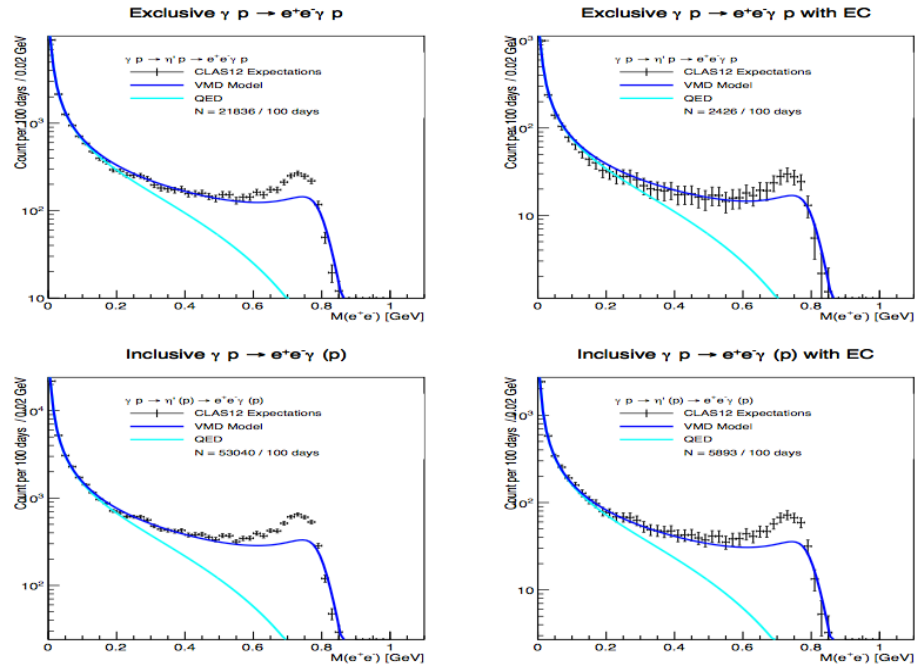


FIGURE 10: Expected count rates for $\eta' \rightarrow e^+e^-\gamma$ in CLAS12